ChemComm

Accepted Manuscript

This article can be cited before page numbers have been issued, to do this please use: S. U. Son, D. Kang, J. H. Ko, J. Choi, K. Cho, S. M. Lee, H. J. Kim, Y. Ko and K. H. Park, *Chem. Commun.*, 2017, DOI: 10.1039/C6CC10005H.

ROYAL SOCIETY OF CHEMISTRY

rsc.li/chemcomm

ROYAL SOCIETY OF CHEMISTRY View Article Online
DOI: 10.1039/C6CC10005H

Journal Name

COMMUNICATION

Dual role of Cu_2O nanocubes as templates and networking catalysts for hollow and microporous Fe-porphyrin networks

rmfoReceived 00th January 20xx,
Accepted 00th January 20xx

DOI: 10.1039/x0xx00000x

www.rsc.org/

Daye Kang,[a] Ju Hong Ko,[a] Jaewon Choi,[a] Kyoungil Cho,[a] Sang Moon Lee,[b] Hae Jin Kim,[b] Yoon-Joo Ko,[c] Kang Hyun Park,[d] and Seung Uk Son*[a]

Cu_2O nanocubes were used for the synthesis of hollow and microporous Fe porphyrin networks (H-MFePN). In the synthesis, Cu_2O nanocubes performed not only as networking catalysts but also as shape controlling templates. MFePN were formed on the surface of Cu_2O nanocubes through azide-alkyne cycloaddition of tetrakis(4-ethynylphenyl) Fe-porphyrin with 1,4-diazidobenzene. H-MFePN showed excellent catalytic activities in carbene insertion to N-H bonds, maintaining the activities in five recycle tests.

Microporous organic networks (MONs) are versatile materials for various applications.[1] For example, due to their porosity, high surface area, and robust stability against most chemical reagents, MONs have been applied as heterogeneous catalysts.[2] Basically, MONs can be prepared by the coupling reactions of rigid building blocks. While various C-C coupling reactions by Pd catalysts have been used for the synthesis of MONs,[3] azide-alkyne cycloadditions (click reactions) based on cheap Cu catalysts are also attractive. As a result, there were reports on the synthesis of MONs based on click reactions.[4] Those MON materials were used as adsorbents and catalysts.[4]

Our research group has shown that the shape control of MONs by template methods can enhance the functional performance of MONs.[5] Generally, MON materials prepared without shape control have shown irregular morphologies with micron sizes.[6] Although such micron-sized MON powders also have porosity and high surface area, substrates should diffuse into MONs to interact with catalytic sites in inner MONs. Moreover, they often show relatively poor dispersion ability in solvents. In contrast, hollow MONs with thin shells (< ~30 nm) can be engineered by template methods and successive template etching.[5] The hollow MONs showed excellent dispersion ability in organic solvents and facile access to catalytic sites in shells, which can enhance catalytic performance.[7]

Recently, the engineering methods of Cu-based nanoparticles have been reported.[8] For example, Cu_2O nanocubes were prepared by a wet chemical synthesis.[9] Copper oxides have been used as catalysts for click reactions.[10] We speculate that shape and size controlled copper oxides can serve as catalysts for the networking of building blocks as well as templates for the engineering of hollow MONs. It is noteworthy that Wang research group recently reported the silica template synthesis of hollow MONs based on click reaction.[4f] In the present work, we report the dual role of Cu_2O nanocubes as networking catalysts and templates for hollow and microporous iron porphyrin networks (H-MFePN) and the catalytic performance of H-MFePN in carbene insertion reaction to N-H bonds of amines.

Fig. 1 shows a synthetic scheme for H-MFePN with the help of dual role of Cu_2O nanocubes.

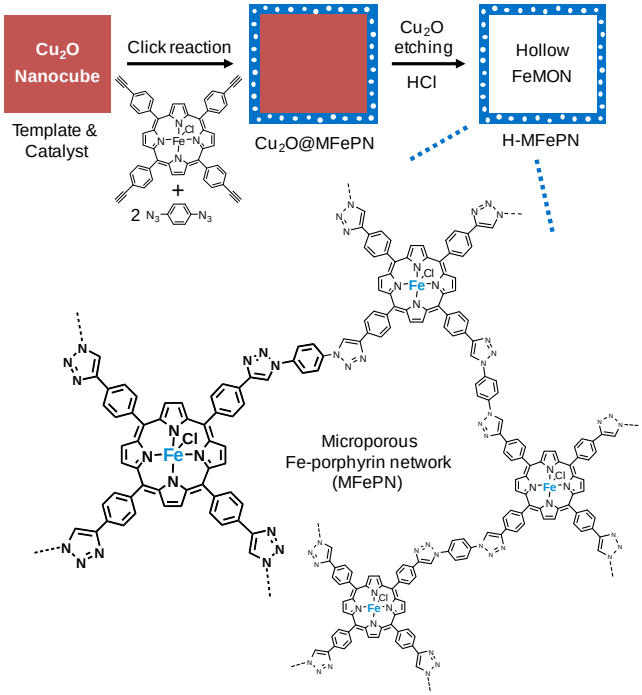

Fig. 1 Synthetic scheme for hollow and microporous Fe-porphyrin networks (H-MFePN).

[a] Department of Chemistry, Sungkyunkwan University, Suwon 16419, Korea
E-mail: sson@skku.edu
[b] Korea Basic Science Institute, Daejeon 350-333, Korea
[c] Laboratory of Nuclear Magnetic Resonance, National Center for Inter-University Research Facilities (NCIRF), Seoul National University, Seoul 08826, Korea
[d] Department of Chemistry, Pusan National University, Busan 46241, Korea

† Electronic Supplementary Information (ESI) available: Experimental procedure, additional TEM and SEM images, and ^1H and ^{13}C NMR spectra of products. See DOI: 10.1039/x0xx00000x

Cu_2O nanocubes were prepared by synthetic procedures in the literature.[9] The average size of Cu_2O was 135 nm. The Cu_2O nanocubes were dispersed in a 9:1 mixture of dimethyl sulfoxide (DMSO) and water. Tetrakis(4-ethynylphenyl) Fe-porphyrin and 2eq. 1,4-diazobenzene were added to the reaction mixture. Simple heating of the reaction mixture induced the formation of microporous Fe-porphyrin networks (MFePN) on the surface of Cu_2O nanocubes. Owing to the catalytic action of surface species, the MFePN were formed only on the surface of Cu_2O nanocubes. Inner Cu_2O of Cu_2O@MFePN was etched by the treatment with HCl solution. The resultant H-MFePNs were characterized by scanning electron microscopy (SEM) and transmission electron microscopy (TEM). (Figs. 2a-e and S1-2 in the ESI)

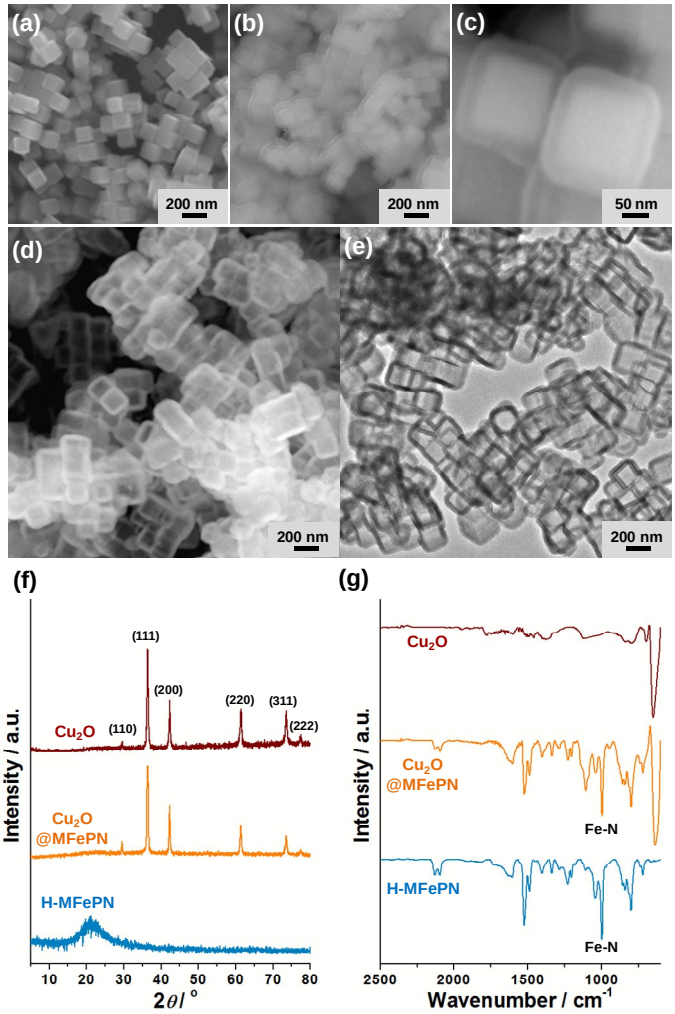

Fig. 2 SEM images of (a) Cu_2O nanocubes, (b-c) Cu_2O@MFePN, and (d) H-MFePN. (e) TEM image of H-MFePN. (f) XRD patterns and (g) IR spectra of Cu_2O nanocubes, Cu_2O@MFePN, and H-MFePN.

As shown in Fig. 2a, Cu_2O nanocubes showed homogeneous shape and size. Cu_2O@MFePN showed the coating layer of MFePN on the surface of Cu_2O nanocubes. (Figs. 2b-c and S2 in the ESI) The SEM and TEM images of H-MFePN showed a hollow inner space and the complete etching of inner Cu_2O materials. (Figs. 2d-e) The average diameter and shell thickness of H-MFePN were measured as 210 and 35 nm, respectively.

Powder X-ray diffraction (PXRD) studies of Cu_2O nanocubes showed (110), (111), (200), (220), (311), and (222) peaks at 29.6, 36.4, 42.3, 61.4, 73.6, and 77.4° of 2θ values, matching well with those of cubic Cu_2O (JCPDS# 78-2076). (Fig. 2f) The PXRD pattern of Cu_2O@MFePN showed the same diffraction peaks of Cu_2O, indicating the structural retention of Cu_2O nanocubes in the networking process of MFePN. The PXRD pattern of H-MFePN revealed amorphous characteristic, which matches well with that of the conventional MON materials synthesized by the catalytic couplings of organic building blocks in the literature.[1-4] The infrared absorption (IR) spectroscopy of Cu_2O@MFePN and H-MFePN showed the vibrational peaks of Fe-N bonds at 999 cm^{-1},[11] supporting the successful incorporation of Fe-porphyrin moieties in the networks. (Fig. 2g)

The physical and chemical properties of H-MFePN were further analyzed by other spectroscopies. The metal porphyrins can be identified by the unique absorption properties of visible lights. Cu_2O has reddish brown color with major absorption in 360~470 nm. The Cu_2O@MFePN and H-MFePN showed new absorption bands at 578 and 623 nm, which are attributable to the Q bands of Fe-porphyrin moieties.[12] (Fig. 3a)

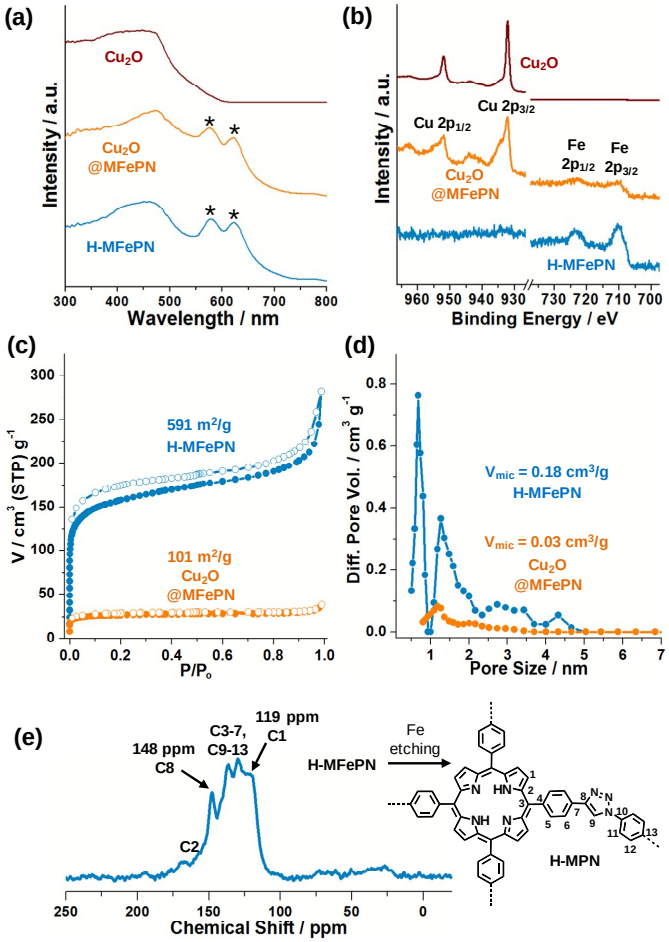

Fig. 3 (a) Absorption and (b) XPS spectra of Cu_2O, Cu_2O@MFePN, and H-MFePN. (c) N_2 sorption isotherm curves at 77K and (d) pore size distribution diagram of H-MFePN and Cu_2O@MFePN based on DFT method. (e) Solid phase ^{13}C NMR spectrum of H-MPN.

View Article Online
DOI: 10.1039/C6CC10005H

X-ray photoelectron spectroscopy (XPS) of Cu_2O and Cu_2O@MFePN showed Cu $2p_{1/2}$ and $2p_{3/2}$ orbital peaks at 951.9 and 932.1 eV, respectively.[10] The XPS spectra of Cu_2O@MFePN and H-MFePN showed Fe $2p_{1/2}$ and Fe $2p_{3/2}$ orbital peaks of Fe-porphyrins at 723.5 and 710.4 eV, respectively.[13] Cu 2p orbital peaks were not detected in the XPS spectrum of H-MFePN, indicating the complete etching of inner Cu_2O of Cu_2O@MFePN. The analysis of N_2 sorption isotherms of H-MFePN by the Brunauer-Emmett-Teller (BET) theory showed a high surface area of 591 m^2/g and microporosity (pore sizes < 2 nm, V_{mic}: 0.18 cm^2/g). (Figs 3c-d) For the nuclear magnetic resonance spectroscopy (NMR), paramagnetic Fe in H-MFePN was etched to form H-MPN by heating in a high concentration HCl solution. Although the ^{13}C peaks of H-MPN were significantly overlapped, the ^{13}C NMR spectrum showed unique triazole and pyrrole carbons at 148 and 119 ppm, respectively. (Fig. 3e)[4a] The elemental analysis showed the existence of 6.0w% nitrogen in H-MFePN. The inductively coupled plasma mass spectroscopy (ICP-MS) indicated the 0.68 mmol Fe/g of H-MFePN.

Recently, iron-based catalysts have been extensively studied due to the environmentally benign nature of nontoxic iron.[14] Moreover, Fe porphyrins attracted the attention of scientists as bio-inspired catalytic systems.[15-16] Considering the high surface area, microporosity, and the existence of Fe-porphyrin moieties, we studied the catalytic performance of H-MFePN towards carbene insertion to amines. Table summarizes the results.

When 1 mol% Fe-porphyrin in H-MFePN was used for the reaction of piperidine with ethyl diazoacetate (EDA), N-H insertion product was formed in 83 and 100 % yield in 1 and 3 min, respectively. (Entries 1 and 2 in Table 1). Without H-MFePN, reaction did not proceed. (Entry 3 in Table 1) *N*,*N*-diethylamine also showed a good yield in reaction with EDA. (Entry 4 in Table 1) In comparison, pyrrole and imidazole showed poor conversion. (Entries 15-16 in Table 1) It has been reported that the carbene insertion to N-H bonds is catalyzed by Fe-porphyrin through the formation of Fischer type Fe-carbene complexes.[16] In this process, amine acts as nucleophile to electron deficient Fischer carbenes. Therefore, more electron rich amines such as piperidine and *N*,*N*-diethylamine showed better yields in carbene insertion reactions. Next, aniline derivatives were screened, showing good activities in carbene insertions. (Entries 5-14 in Table 1) As anilines become more electron-rich, the yields of double N-H insertion product gradually increased. This also can be rationalized considering the increased nucleophilicity of more electron-rich anilines.

We tested the recycle ability of H-MFePN. As shown in Entries 7-11 and Fig. 4a, H-MFePN showed excellent retention of catalytic activity and selectivity in at least five recovery cycles. The H-MFePN recovered after five successive cycles was further investigated by various methods. (Figs 4b-e) As shown in Figs 4b-c, the original morphologies of H-MFePN completely were retained after five catalytic cycles. In addition, XPS and absorption spectroscopy supported the retention of electronic situation of Fe and the Q bands of Fe-porphyrins in the recovered H-MFePN, indicating the robust properties of H-MFePN. (Figs 4d-e).

Table 1. Carbene insertion to N-H bonds catalyzed by H-MFePN.[a]

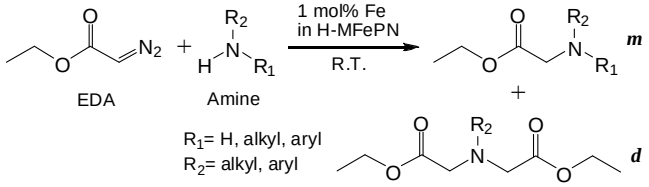

Entry	Amine	Product	Yield[b] (%)	*m*/*d*[c] (%)
1[d]		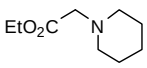	83	100/0
2			100(98)	100/0
3[e]			0	-
4		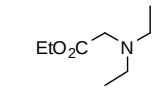	100(87)	100/0
5	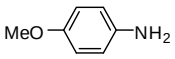	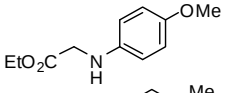	100[f]	81/19
6	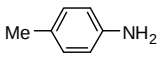	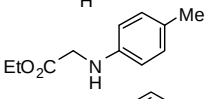	100(74)	90/10
7	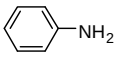	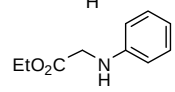	100(80)	93/7
8[g]			100	93/7
9[h]			100	92/8
10[i]			100	93/7
11[j]			100	95/5
12	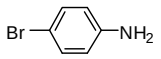	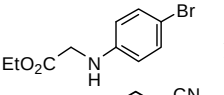	100(84)	98/2
13	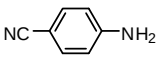	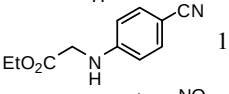	100(74)[k]	99/1
14	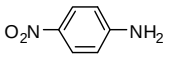	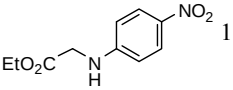	100(59)[l]	100/0
15		-	trace	-
16		-	trace	-

[a] Reaction conditions: H-MFePN (1 mol% Fe-porphyrins for EDA, 7.0 mg, 4.8 μmol Fe-porphyrins based on the ICP-MS analysis), amine (0.48 mmol), EDA (0.48 mmol), acetone (3 mL), argon, r.t., 3 min. [b] Conversion yields of EDA based on ^1H NMR (1,4-Dimethoxybenzene was used as an internal standard). The isolated yields of the single N-H insertion products are indicated in parenthesis. [c] Selectivity: the molar ratios of single N-H insertion product (*m*), double N-H insertion product (*d*). [d] The reaction time was 1 min. [e] No catalyst was used. [f] The major product was decomposed during silica column chromatography. [g] The catalyst recovered from Entry 7 was used. [h] The catalyst recovered from Entry 8 was used. [i] The catalyst recovered from Entry 9 was used. [j] The catalyst recovered from Entry 10 was used. [k] The maximum isolated yield of major product was calculated as 77% due to the formation of EDA dimer. [l] The maximum isolated yield of major product was calculated as 63% due to the formation of EDA dimer.

Heterogeneous catalytic systems bearing Fe-porphyrins for the carbene insertion to N-H bonds are rare.[17] Moreover, H-MFePN (the complete conversion of aniline in 3 min, 1 mol% Fe-porphyrins, r.t.) was much superior to heterogeneous systems (the complete conversion of aniline in 20 or 30 min, 1 mol% Fe-porphyrins, r.t.) in the literature,[17] which may result from the short diffusion pathway of substrates and good dispersion ability of H-MFePN.

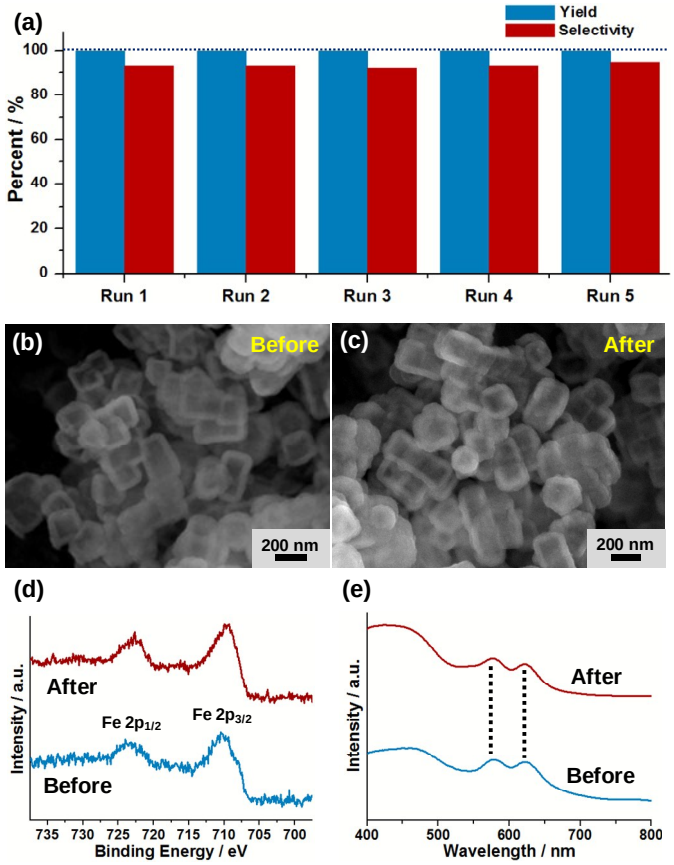

Fig. 4 (a) Recycle tests (Entries 7-11 in Table 1) of H-MFePN catalysts in the reaction of EDA with aniline. (b) SEM images, XPS, and absorption spectra of H-MFePN before and after five catalytic cycles.

In conclusion, this study introduces the efficient synthetic strategy for the shape-controlled MON materials, in which hollow and microporous Fe-porphyrin networks were successfully engineered utilizing Cu_2O nanocubes as templates and networking catalysts. We believe that this synthetic strategy is extendable to more various hollow and functional MONs through screening of the tailored building blocks.

Acknowledgements

This research was supported by Basic Science Research Program (2016R1E1A1A01941074) through the NRF of Korea funded by the Ministry of Science, ICT and Future Planning.

Notes and references

1 Reviews: (a) Y. Xu, S. Jin, H. Xu, A. Nagai and D. Jiang, *Chem. Soc. Rev.* 2013, **42**, 8012-8031; (b) R. Dawson, A. I. Cooper and D. J. Adams, *Prog. Poly. Sci.* 2012, **37**, 530-563; (c) F. Vilela, K. Zhang and M. Antonietti, *Energy Environ. Sci.* 2012, **5**, 7819-7832; (d) A. Thomas, *Angew. Chem. Int. Ed.* 2010, **49**, 8328-8344; (e) N. B. McKeown and P. M. Budd, *Chem. Soc. Rev.* 2006, **35**, 675-683.

2 Reviews: (a) Y. Zhang and J. Y. Ying, *ACS Catal.* 2015, **5**, 2681-2691; (b) P. Kaur, J. T. Hupp and S. T. Nguyen, *ACS Catal.* 2011, **1**, 819-835; (c) Y. –L. Wong, J. M. Tobin, Z. Xu and F. Vilela, *J. Mater. Chem. A* 2016, **4**, 18677-18686: (d) L. Pan, M. –Y. Xu, L. –J. Feng, Q. Chen, Y. –J. He and B. –H. Han, *Polym. Chem.* 2016, **7**, 2299-2307; (e) S. Bhunia, B. Banerjee and A. Bhaumik, *Chem. Commun.* 2015, **51**, 5020-5023; (f) S. Xu, K. Song, T. Li and B. Tan, *J. Mater. Chem. A* 2015, **3**, 1272-1278.

3 (a) J. –X. Jiang, F. Su, A. Trewin, C. D. Wood, N. L. Campbell, H. Niu, C. Dickinson, A. Y. Ganin, M. J. Rosseinsky, Y. Z. Khimyak and A. I. Cooper, *Angew. Chem., Int. Ed.* 2007, **46**, 8574-8578; (b) J. –X. Jiang, F. Su, A. Trewin, C. D. Wood, H. Niu, J. T. A. Jones, Y. Z. Khimyak and A. I. Cooper, *J. Am. Chem. Soc.* 2008, **130**, 7710-7720.

4 (a) J. R. Holst, E. Stöckel, D. J. Adams and A. I. Cooper, *Macromolecules* 2010, **43**, 8531-8538; (b) O. Plietzsch, C. I. Schilling, T. Grab, S. L. Grage, A. S. Ulrich, A. Comotti, P. Sozzani, T. Muller and S. Bräse, *New J. Chem.* 2011, **35**, 1577-1581; (c) P. Pandy, O. K. Farha, A. M. Spokoyny, C. A. Mirkin, M. G. Kanatzidis, J. T. Hupp and S. T. Nguyen, *J. Mater. Chem.* 2011, **21**, 1700-1703; (d) L. Li, H. Zhao and R. Wang, *ACS Catal.* 2015, **5**, 948-955; (e) H. Zhong, C. Liu, Y. Wang, R. Wang and M. Hong, *Chem. Sci.* 2016, **7**, 2188-2194; (f) L. Li, C. Cui, W. Su, Y. Wang and R. Wang, *Nano. Res.* 2016, **9**, 779-786.

5 (a) N. Kang, J. H. Park, M. Jin, N. Park, S. M. Lee, H. J. Kim, J. M. Kim and S. U. Son, *J. Am. Chem. Soc.* 2013, **135**, 19115-19118; (b) J. Chun, S. Kang, N. Park, E. J. Park, X. Jin, K. –D. Kim, H. O. Seo, S. M. Lee, H. J. Kim, W. H. Kwon, Y. –K. Park, J. M. Kim, Y. D. Kim and S. U. Son, *J. Am. Chem. Soc.* 2014, **136**, 6786-6789; (c) S. Kang, J. Chun, N. Park, S. M. Lee, H. J. Kim and S. U. Son, *Chem. Commun.* 2015, **51**, 11814-11817.

6 (a) A. Laybourn, R. Dawson, R. Clowes, T. Hasell, A. I. Cooper, Y. Z. Khimyak and D. J. Adams, *Polym. Chem.* 2014, **5**, 6325-6333; (b) B. Kim, N. Park, S. M. Lee, H. J. Kim and S. U. Son, *Polym. Chem.* 2015, **6**, 7363-7367.

7 (a) N. Park, Y. N. Lim, S. Y. Kang, S. M. Lee, H. J. Kim, Y. –J. Ko, B. Y. Lee, H. –Y. Jang and S. U. Son, ACS Macro Lett. 2016, 5, 1322-1326; (b) J. H. Ko, N. Kang, N. Park, H. –W. Shin, S. Kang, S. M. Lee, H. J. Kim, T. K. Ahn and S. U. Son, *ACS Macro Lett.* 2015, **4**, 669-672.

8 M. B. Gawande, A. Goswami, F. –X. Felpin, T. Asefa, X. Huang, R. Silva, X. Zhou, R. Zboril and R. S. Varma, *Chem. Rev.* 2016, **116**, 3722-3811.

9 I. –C. Chang, P. –C. Chen, M. –C. Tsai, T. –T. Chen, M. –H. Yang, H. –T. Chiu and C. –Y. Lee, *CrystEngComm* 2013, **15**, 2363-2366.

10 K. Chanda, S. Rej and M. H. Huang, *Chem. Eur. J.* 2013, **19**, 16036-16043 2

11 Z. –C. Sun, Y. -B. She, Y. Zhou, X. –F. Song and K. Li, *Molecules* **2011**, *16*, 2960-2970.

12 M. Jahan, Q. Bao and K. P. Loh, *J. Am. Chem. Soc.* 2012, **134**, 6707-6713.

13 K. M. Kadish, L. A. Bottomley, J. G. Brace and N. Winograd, *J. Am. Chem. Soc.* 1980, **102**, 4341-4344.

14 K. Gopalaiah, *Chem. Rev.* 2013, **113**, 3248-3296.

15 (a) L. K. Baumann, H. M. Mbuvi, G. Du and L. K. Woo, *Organometallics* 2007, **26**, 3995-4002; (b) I. Aviv and Z. Gross, *Synlett* 2006, **6**, 951; (c) I. Aiv and Z. Gross, *Chem. Eur. J.* 2008, **14**, 3995-4005.

16 D. A. Sharon, D. Mallick, B. Wang and S. Shaik, *J. Am. Chem. Soc.* 2016, **138**, 9597-9610.

17 (a) J. Yoo, N. Park, J. H. Park, J. H. Park, S. Kang, S. M. Lee, H. J. Kim, H. Jo, J. -G. Park and S. U. Son, *ACS Catalysis* 2015, **5**, 350-355; (b) L. Xu, M. –K. Zhai, F. Wang, L. Sun and H. –B. Du, *Dalton Trans.* 2016, **45**, 17108-17112.